Available online at www.sciencedirect.com
SCIENCE DIRECT
Computers and Electronics in Agriculture 48 (2005) 63–74
Computers and electronics in agriculture
www.elsevier.com/locate/compag

A transportable fluorescence imagining system for detecting fecal contaminants

Alan M. Lefcourt *, Moon S. Kim, Yud-Ren Chen

Instrumentation and Sensing Laboratory, U.S. Department of Agriculture, Agricultural Research Service, Building 303 Powder Mill Road, Beltsville, MD 20705, USA

Received 9 August 2004; received in revised form 19 January 2005; accepted 25 January 2005

Abstract

Feces are the primary source of many pathogenic organisms that can potentially contaminate agricultural commodities. Feces generally contain chlorophyll a and related compounds due to ingestion of plant materials. Fluorescent responses of these compounds to appropriate excitation can mark the presence of feces on animal carcasses, or on fruits or vegetables. We describe a transportable imaging system for detecting fecal contamination. The primary components of the system are a UV light source, an intensified camera with a six-position filter wheel, and software for controlling the system and automatically analyzing images. To test the system, diluted dairy feces were applied to surfaces of red delicious apples using stencils or a pipette. Comparisons of test results using a definitive set of four red-band filters demonstrated that the contrast between fluorescence responses of treated and untreated apple surfaces decreased with increasing wavelength, and was 25% greater at 668 compared to the best results obtained at 678, 685, or 700 nm. Using images acquired at 668 nm, automated algorithms based on either threshold or edge detection were 100% successful in detecting stenciled apples and 1:10 dilution spots applied with pipette, which contained approximately 300 ng of dry matter. In a separate test, sets of feces-treated apples were washed at hourly intervals and then imaged. The contamination sites could not be detected when the contact time was less than 4 h, while 5 h of contact was sufficient to establish consistent fluorescence responses in images. Use of a modified system as a teaching tool demonstrated the robustness of the system and promoted public awareness that fecal contamination invisible to the naked eye can easily be detected with appropriate instrumenta-

* Corresponding author. Tel.: +1 301 504 8450; fax: +1 301 504 9466.
E-mail address: alefcour@anri.barc.usda.gov (A.M. Lefcourt).

0168-1699/$ – see front matter. Published by Elsevier B.V.
doi:10.1016/j.compag.2005.01.002

tion. There are many potential uses for this system, including studying the efficacy of apple washing systems.
Published by Elsevier B.V.

Keywords: Fluorescence; Multispectral imaging; Food safety; Fecal contamination

1. Introduction

Feces are the primary source of pathogenic *Escherichia coli* contamination of agricultural commodities and, as there is no definitive assay for fecal contamination, FDA (2001) and FSIS (2004) use the presence of generic *E. coli* as an indicator for fecal contamination. The adverse health risks of *E. coli* in foods are well documented (Armstrong et al., 1996; Hui, 2001; Mead et al., 1999). Feces can also be the source of many other types of pathogenic organisms, including parasites (Blackburn and McClure, 2002; Hui, 2001). The authors have demonstrated that fluorescence can be a very sensitive method for detecting feces (Kim et al., 2002, 2003; Lefcourt et al., 2003), and that fluorescence responses of feces from different animal species are similar (Kim et al., 2003).

We present the design, construction, and testing of a transportable system for automatically detecting fecal contamination on agricultural products ranging in size from berries to chicken carcasses. Prior results demonstrated that fecal contamination on apples can be detected by measuring fluorescence in the red-band in response to UV excitation (Kim et al., 2002, 2003; Lefcourt et al., 2003). In this study, an intensified camera with a filter wheel was used for sensitivity and to allow comparison of fluorescence responses using different filters. Apples were used as the test matrix because the FDA has indicated a specific need for a system to detect apples contaminated with feces (FDA, 2001). Prior observations suggested that imaging using shorter wavelengths in the red-band might improve the contrast between fluorescence responses of feces-treated and untreated apple surfaces. The first objective of this study is to determine the optimal waveband in the red region for detecting fecal contamination on apples. This question is addressed by imaging contaminated apples using a definitive set of red-band filters and comparing contrast ratios between contaminated and uncontaminated apple surfaces.

One potential use of this system would be to measure the efficacy of different methods of washing fruits during processing. However, the authors have demonstrated that a fluorescence response resulting from to fecal contamination can be detected on apples even after the feces are removed from the apple by washing and brushing (Lefcourt et al., 2003). An induced fluorescence response due to fecal contact could interfere with experiments to test the efficacy of washing. The second objective is to determine how long the feces must be in contact with an apple before the contamination site can be detected after the apple is washed. This question is addressed by washing contaminated apples at hourly intervals and looking for fluorescence responses in images of the washed apples.

The education of the public concerning safe food handling and the difficulty of detecting fecal contamination is also a public health issue. One goal in the design of the transportable system was the use of the system for public demonstrations to show that fecal contamination invisible to the human eye could be detected with appropriate instrumentation. Thus, the

third objective is to demonstrate the use of the system in a public setting. Successful use of the system in a public setting will demonstrate the hardiness of the system while simultaneously raising public awareness of the difficulty of detecting fecal contamination, and hence, the need for cleanliness.

2. Methods

2.1. Camera

The camera is a second-generation intensified camera (ICCD) with a six-position filter wheel (Model IMC-201-U-3, Xybion Electronics Systems). Four red-band, one blue-band, and one green-band filter were used in this study (Table 1). The red-band filters were selected to address the issue of which waveband was best for single-band detection of feces on apples. The wider bandwidth of the 700 nm filter was meant to encompass both the primary and secondary chlorophyll a fluorescence emissions peaks. The other two filters were selected as prior studies suggested that ratios of red-band to blue- or green-band images could improve detection, in part by correcting for non-uniform illumination when a pulsed laser was used for illumination (Lefcourt et al., 2003). The camera is powered by an external 12 V dc power source and has a RS-170 output with a 30 Hz refresh rate along with a separate digital output encoding the position of the filter wheel. An image is acquired using a frame-grabber with ten-bit resolution, adjustable window dimensions, and selectable gain and bias (Model PCI-1409, National Instruments). The selectable gain and bias can be used to produce effects similar to software-based histogram stretching; the principle difference is that the conversion is done before the image is digitized, which allows the full 10-bit hardware resolution to be used to represent the "stretched" image. Continuous rotation of the filter wheel allows sequential acquisition of six band images at a rate of five images/s per band (Park and Chen, 2001). However, continuous rotation limits the maximum exposure time for individual images to around 4 ms. For this study, the filter wheel was selectively locked at single positions to allow exposure time to be increased up to a maximum of 33 ms. The intensifier gain can be set from 1 to 100%. In use, the ICCD gain and exposures were set to represent half of the expected dynamic range of the sample set. As an example, for fluorescence imaging in a dark environment using the 668 nm filter, the exposure time and gain are set to 33 ms and 80%, respectively. Operating parameters are normally set using a serial interface, but can also be set via a keypad on the back of the

Table 1
Specifications of interference filters for the six-position filter wheel

Filter number	Wavelength (nm)	FWHM (nm)	Transmittance (%)
1	450	40	45
2	550	40	75
3	668	10	75
4	678	22	75
5	685	10	75
6	700	40	75

camera. The camera allows display of user selected operating parameters, including filter wheel position, to be superimposed as text on actual images. The display location of the text is selectable. The operating parameters can also be expressed as a barcode on the leading edge of the image or downloaded through the serial interface.

2.2. Lighting

A UV-A light source is used for illumination. Four fluorescent light fixtures (Model EA-180/12, Spectroline) are located around the camera. For each unit, a bandpass filter (5 cm × 15 cm, UG-1) is used to restrict output to between 300 and 400 nm. The fixtures are attached to a square aluminum frame (44 cm × 44 cm), angled at 45° towards the center, and wired in parallel to an external 12 V dc power source. The distance between the lights and the imaging area is about 40 cm. The lighting is near uniform except for a slight gradient in the vertical dimension that results because of the camera size and mounting constraints, and an off-center location of the lens on the camera body (see Dark current and flat-field corrections, below).

2.3. System

The lighting fixtures and camera are mounted on the same frame and face downward. The frame is supported by four aluminum posts with two posts on each side of the frame, which yields lateral dimensions of 49 cm × 44 cm. The lights are approximately 25 cm and the camera face is about 36 cm above the surface. With the appropriate C-mount lens, the image area can range from an area sufficient to encompass an apple to a chicken carcass. The frame structure is normally housed in a portable light-tight enclosure (60 cm × 60 cm × 74 cm in height) with black internal walls, a magnetically sealed door, and a baffled exhaust fan. Because of the limited focal distance, the use of a brass lens spacing ring is sometimes necessary to allow proper focusing at the costs of decreased depth-of-field and possible fisheye aberration. For apples, a 25 mm, 1:1.4, 1-in. lens (Rainbow) and a 1.25 mm thick brass lens spacing ring is used. By using an *f*-stop of 2.8, the entire hemisphere surface of an apple can be brought into focus. The current system is a compromise that balances incident light intensity, overall system size, potential range of target size, pixel dimension of images, and image quality.

2.4. Data acquisition and analyses

The camera is controlled, and data are collected and analyzed using a PC running Microsoft Windows XP Professional® and Visual Basic Version 6®. Serial communication is used to select filters, exposure times, and intensifier gains. Image acquisition uses an ActiveX Control (CWIMAQ, National Instruments) to set the gain and bias of the analog to digital converter, to set the image window, and to transfer individual images to digital arrays. By splitting the RS-170 signal, the real time camera output can also be displayed on a video monitor.

In use, the imaging window is set to 640 × 480 to allow capture of operating parameters superimposed as text along the top of the image. Software is used to select a region of

interest for image display and analyses, and to select the filters to be used and the number of sequential images per filter to average. When multiple filters are selected, the filter wheel is moved sequentially from filter to filter; a 3 s delay is introduced at each transition to allow the camera to lock the filter wheel in place. At each filter stop, the selected number of images are acquired and averaged. Averaging four images is optimal in terms of balancing improved signal to noise ratio with net image acquisition time. Once all operating parameters are selected, a single click of a button-icon will acquire an image or set of images and, if enabled, the acquired data can be automatically subjected to two user-defined detection algorithms. Alternatively, acquired images are immediately available for analysis using a range of image manipulations (e.g., brightness, contrast, normalization, exponential scaling, linear combination of images, and ratios of two images) and filters (e.g., spatial, geometric, morphological, edge, and threshold, Weeks, 1996). Raw or transformed images can be viewed as images, false color images, or histograms. Automated detection is accomplished by subjecting acquired data to a selected series of transformations and then applying a threshold to the resultant image. Transformations used for the two automated detection algorithms are selected by entering the appropriate codes in a text box. The final detection threshold can be set manually or automatically. The automated threshold is set based on the zeroth- and first-order cumulative moments of the gray-level histogram (Otsu, 1979), or a derivation where moments are calculated based on a priori selected bounds in the histogram. The total number of pixels above a selected threshold and within a selected pixel distance of each other is used to determine whether a positive response exists. For visualization of detection, all pixels with intensities greater than or equal to the threshold are colored red and are superimposed on the original image; the actual number of pixels for each group of pixels within a selected pixel distance of each other is listed. In general, the detection threshold can be iterated for a set of test images to determine the number of correctly identified contamination sites and the number of false positives as a function of the threshold level. This information can be used to select a detection threshold. For this study, a wide range of detection thresholds could effectively detect contamination sites on unwashed apples (see Modifications for use in public displays, below). Automated image acquisition and detection generally takes 3 to 60 s depending on the number of filters used, and the number and types of transformations selected.

2.4.1. Dark current and flat-field corrections (third level heading)

A selectable option allows for images to be corrected for dark current, non-uniformity, or both using selected dark current and flat-field reference images. Using filter 1 or 2 to maximize light throughput, a dark current image is obtained by acquiring an image with the UV light source switched off and a flat-field reference image is acquired using a reference medium (Epson® Photo Quality Ink Jet Paper). To correct for dark current, pixel values for the dark current image are subtracted from corresponding image values; resulting values less than zero are set to zero. To correct for non-uniformity, individual pixel correction factors are calculated by determining the mean intensity for pixels in the selected region of interest for the dark current-corrected flat-field image and then ratioing individual pixel intensities to this mean value. The correction factors are assumed to be filter independent.

2.4.2. Linear image normalization (third level heading)

A selectable option is to correct images for uniform power by using a linear function to map pixel intensities based on the cumulative intensity histogram within the selected region of interest. The intensity corresponding to the 3% histogram level is generally mapped to an intensity of 20 and the 75% level to 65. Resulting values less than 0 or greater than 1023 are set to 0 or 1023, respectively. The purpose of this procedure is to address differences among apples in terms of natural fluorescence responses by taking advantage of the a priori knowledge of the approximate areas of an image occupied by the background and by an apple. The lower mapping point is in the background area and the upper point is representative of the median fluorescence response of the apple. Using histogram stretching is less effective as the upper mapping point is adversely impacted by the variability of the responses of contamination sites.

2.4.3. Contrast calculations (third level heading)

Contrast ratios between contaminated and uncontaminated areas for individual images were calculated by dividing the average intensity within a contaminated area by the corresponding average intensity within the remaining uncontaminated area. First, for an individual image, a region of interest was selected that encompassed the apple. Second, a threshold function was used to mask the apple from the background. Third, a second threshold function was used to mask the contaminated areas from the uncontaminated apple surface. These thresholds were used to determine the exact number of pixels to be used to represent the background, the uncontaminated apple surface, and the contaminated area. The selection of thresholds was done empirically by visual observation. To eliminate any bias resulting from the threshold selections, the same pixel counts for selected areas were used to analyze images of an individual apple regardless of the filter used to acquire the image. Contrast ratios for each of the four red-band images associated with each apple were calculated by applying the pixel count thresholds to corresponding intensity histograms. Pixels in histogram bins at pixel count thresholds were apportioned so that the number of background, uncontaminated, and contaminated pixels were identical for each set of four red-band images. To allow comparison of relative contrasts among apples by filter wavelength, relative contrast ratios were calculated by dividing contrast ratios for all four red bands for an individual apple by the ratio for the 668 nm filter. Additionally, coefficients of variation for individual images were calculated for intensities within uncontaminated and contaminated areas.

2.4.4. Modifications for use in public displays (third level heading)

A separate Visual Basic form was created to allow the system to be used for public displays. The form uses images and audio to impart information about fecal contamination and the problems of detecting apples contaminated with feces. Audio messages are also displayed as text. Following this introduction, the computer asks public users to point to an apple for testing. To eliminate the possibility of the public coming into contact with feces, a technician places the selected apple in the system. Users are then led to select on icon that initiates image acquisition using the 668 nm filter. The image, once acquired, is subject to the uniform power transform and displayed. Simultaneously, a layman's explanation concerning the underlying theory for threshold and for edge detection is initiated. At the end of the explanation, icons for starting both detection methods are displayed and an

audible message encourages users to try both detection methods. For edge detection, a 5×5 Prewitt filter is used (Weeks, 1996). For both detection methods, contaminated areas are determined by summing the number of pixels that exceed the appropriate detection threshold and are within a distance of 10 pixels of each other. Contaminated areas are overlaid on the original image in red as indicated in an audio message. For this study, the contamination sites on the unwashed apples could be detected without error across a wide range of detection thresholds; the difference being the number of pixels detected. Detection thresholds were arbitrarily set to approximately the middle of the range of viable values, which was 130 for threshold detection and 600 for edge detection.

2.5. Feces application to apples

Fresh feces were acquired from the BARC (Beltsville Area Research Center) dairy and diluted by weight with distilled water. The dry matter content of the feces was determined to be 15.8% by drying three samples of feces to constant weight in a 60 °C oven. The diluted feces were applied to Red Delicious apples using stencils or as drops using a 20 μl pipette. Apples where hand-picked at a local Maryland farm and stored in an apple refrigerator at 3 °C prior to use and when not in use. Tests indicated that repeated cooling and storage over a period of weeks had no effect on fluorescence responses as long as apples were allowed to warm prior to imaging so that no condensation was apparent on the apples.

A single stencil made from a gummed-label was applied and then a pattern of 1:10 diluted feces was painted over the open area of the stencil to create an appliqué. After 24–48 h, the stencil was removed, which also removed essentially all visible sign of the applied feces. Specific stencils used include the “poison face”, the ARS (Agricultural Research Service) logo, and the abbreviations “USDA” and “ISL”. A total of 20 stenciled apples were created, four for each of five stencil types. For the public display, the three of the four apples of each of the four stencil-types mentioned above that had the clearest appliqués were used along with four untreated apples. The fifth stencil-type was not used for the public display as the stencil had too many fine details that were blurred in the appliqués.

2.5.1. Apples used for study on contact time (third level heading)

Two 1:10 and two 1:100 drops were applied to the surface of 20 apples. Every hour after application starting at the second hour, feces were removed from a group of four apples by rinsing the apples in water for one min. The apples were imaged prior to washing and after they were allowed to dry. Based on the dry matter content, 1:10 and 1:100 treatment drops contained about 300 and 30 ng of solids, respectively.

3. Results and discussion

3.1. Imaging characteristics

The dynamic range of the 10-bit images was maximized by adjusting the gain and the bias of the analog to digital converter. Appropriate adjustment of these parameters can reduce effective dark current levels to very low levels. In contrast, flat-field reference images

showed considerable variation on a pixel-by-pixel basis with a slight trend from darker to lighter along the vertical axis. The relative difference between the largest and the smallest correction factor within a selected region of interest was generally around 25%. The non-uniformity of the correction factors along the vertical axis is probably due to misalignment of the light source and the camera lens. Contributing factors to the misalignment are the use of a single frame to mount both the camera and the lights, and the off-center position of the lens aperture on the camera body. Use of a wider and taller enclosure along with an independent frame to mount the camera would alleviate this problem. Increased height would also allow for increased depth-of-field. The trade-off would be a slightly smaller field of view if the current lighting scheme was used, or a decrease in incident light intensity and a possible decrease in lighting uniformity if the lights were spread-out to allow a larger field-of-view.

Functionally, dynamic range was maintained by adjusting the exposure and intensifier gain of the camera. In general, noise levels are reduced by using the maximum exposure time available (33 ms) and adjusting the gain appropriately. There is an additional consideration for using the current camera if multiple filters are used. The camera allows different exposure times to be assigned to each filter; however, only one gain can be set. It is possible to change both exposure and gain settings for each filter by resetting the camera operating parameters each time the filter wheel is moved; however, the reset procedure is time consuming. Fundamentally, a choice has to be made between complete control of settings using time consuming procedures or using a single gain and varying exposure times. For this study, a single gain was used and exposure times were indexed to the filter of primary interest.

3.2. Detection of feces

The contamination sites on all stenciled apples were apparent in images subjected to the uniform power transformation (Fig. 1). The purpose of this transformation was to eliminate differences due to the natural variation in fluorescence responses among apples. Contrast between contaminated and uncontaminated surface areas was greatest at 668 nm. The peak fluorescence response for feces occurs at 675 nm (Kim et al., 2003) while the peak response for apples occurs at 685 nm (Kim et al., 2002). These findings suggested that detection of contamination could be enhanced by imaging using a wavelength just shorter than 675 nm. In this study, responses for a definitive set of filters were compared. For detection of fecal contamination, the contrast between average intensities for contaminated and uncontaminated areas was 25% greater at 668 nm compared to the best results for the other tested wavelengths (Table 2). As the coefficients of variation were similar, just greater than 1, for all contaminated and uncontaminated areas, this increased contrast can be interpreted as increased sensitivity. As a consequence of this finding, only images acquired using the 668 nm filter was analyzed in the remainder of the experimental trials.

A prior study indicated that edge detection followed by threshold detection was more sensitive than simple threshold detection for detecting contamination sites on apples (Lefcourt et al., 2003). For this reason, both threshold and edge detection schemes were implemented as the algorithms used for automated detection of fecal contamination. An example showing the results of both detection schemes is shown in Fig. 2. For the apples with appliqués, con-

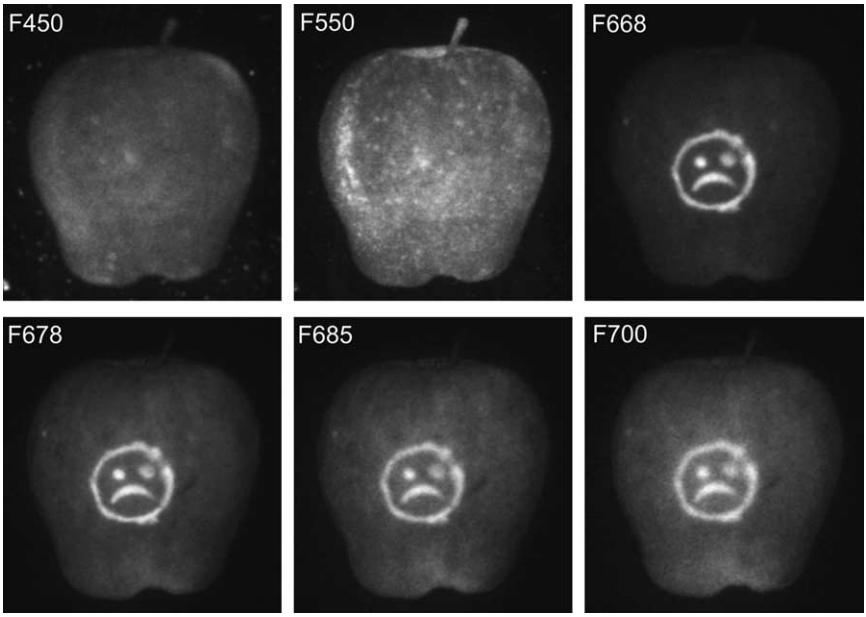

Fig. 1. Examples of images of a single apple using the six filters as indicated. The poison face appliqué was produced by applying a stencil to a *Red Delicious* apple and than painting the stencil with diluted dairy manure. The contrast ratios of average intensities for contaminated to uncontaminated areas were 3.89, 2.85, 2.48, and 2.40 for the 668, 678, 685, and 700 nm images, respectively. The speckles in the background of the 450 and 550 nm images are due to dust particles on the black velour background.

tamination sites were large and, using the 668 nm images, all contamination sites could be detected using a single threshold and counting only contiguous pixels above the threshold. Selection of the exact detection threshold was not critical due to the large contrast at 668 nm between contaminated and uncontaminated areas.

3.3. Affect of feces-apple contact time

A representative example where feces were applied to an apple and then washed off 6 h later is shown in Fig. 3. As is apparent, the 6 h contact time was sufficient to allow identification of the contamination sites when the apple was subsequently imaged using the

Table 2
Relative contrast ratios referenced to the contrast ratio at 668 nm

	Filter wavelength (nm)			
	668	678	685	700
Maximum	1.00	0.83	0.70	0.69
Minimum	1.00	0.71	0.69	0.57

For individual apples, relative contrast ratios always showed a monotonic decrease as the filter wavelength increased.

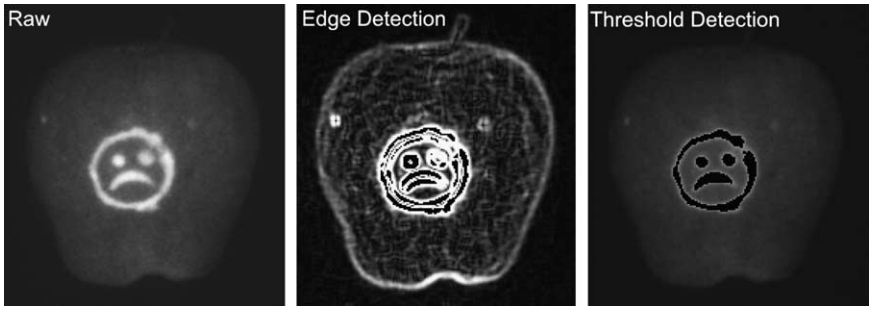

Fig. 2. Representation images produced by the automated detection algorithms based on threshold and edge detection. Detected areas shown in black here are displayed on the computer monitor in red. The raw image was taken using the 668 nm filter.

668 nm filter. The magnitude of responses from 1:100 dilution spots were marginal in terms of automated detection as described above; however, automated detection of the 1:100 spots is possible if detection thresholds are lowered to allow some false positive readings. Even so, detection of all 1:100 spots that were visible in images could not be accomplished using a single threshold. The edge detection algorithm seemed to be a little more sensitive than simple threshold detection; however, the number of detected 1:100 spots was not different. No attempt was made to categorize trade-offs among detection methods, thresholds, and numbers of false positives as the goal was simply to determine the contact time necessary to induce a fluorescence response that was sustained after an apple were washed. The inability to quantify the treatment due to the variability and low level of responses after minimal contact times and the limited number of apples tested precluded more detailed analyses. The tabulated results indicate that 5 h contact time was necessary and sufficient to induce visible responses in apple images due to contact with either 1:10 or 1:100 dilutions of feces

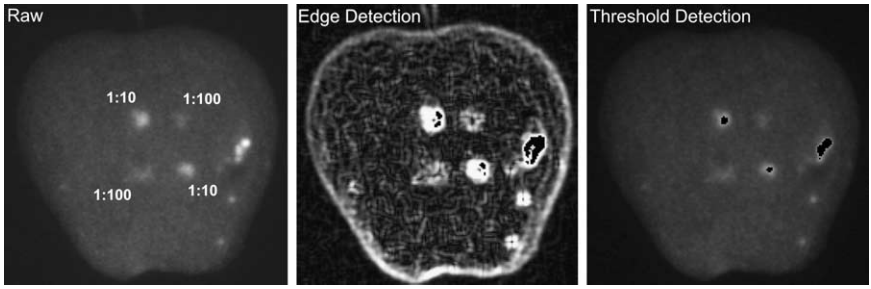

Fig. 3. A representative image showing residual fluorescence responses after 1:10 and 1:100 dilutions of dairy feces were allowed to adhere to the apple for 6 h before the apple was washed. The image was taken after the apple was allowed to air dry. The bright spot on the right of the apple appeared to be due to a prior injury. Injury often causes a localized increase in chlorophyll content, which produces a response similar to the response due to feces. The raw image was taken using the 668 nm filter. Areas detected using the automated threshold and edge detection algorithms are shown in black. For both detection methods, with the detection thresholds set to exclude non-specific fluorescence responses, only the 1:10 dilution spots and the injury site were detected.

Table 3
Number of 20 μl treatment spots visible on apple surfaces after washing the apples as a function of feces-apple contact time

Time after application (h)	Applied feces concentration	
	1:10 dilution	1:100 dilution
6	8/8	7/8
5	8/8	7/8
4	2/8	2/8

Results for images taken for the 2 and 3 h treatment groups are not shown, as no treatment effects were visible in associated images.

(Table 3). Contact times of less than 4 h yielded no visible fluorescence responses that could be attributed to the application of feces.

3.4. Public display

The use of stencils allowed production of contaminated apples that were visually appealing to the public, and particularly children. The only real problem with using the stencils is poor adherence of a "flat" stencil to the curved, waxy, apple surface. Poor adhesion results in seepage of the feces under the stencil, which causes edges of appliqués to appear blurry when the apples are imaged. The adhesion problem can be mitigated by waiting a few minutes after applying the stencil and then checking for good adherence. It is also possible to treat excess apples and to subsequently discard apples where the appliqué is not crisp.

The system was used successfully as a hands-on public display at the annual BARC Field Day. The most popular appliqué was the poison face (Fig. 2). Participants selected an apple, which was placed in the imagining system by an experienced operator. This procedure guaranteed that the public did not come into direct contact with a contaminated apple and assured that the apples were correctly positioned to show the contamination site. Throughout the day, hundreds of random tests were performed using the 12 contaminated and 4 untreated test apples. The system performed flawlessly, correctly identifying the contamination sites using either automated detection scheme. No contamination was every detected on the untreated apples. The ability of the system to function under such demanding conditions, where ambient temperature ranged from 19 to 30 °C, demonstrates the hardiness of the system.

4. Conclusion

A robust, transportable, and sensitive fluorescence imaging system has been developed. The system can image agricultural products ranging in size from berries to chicken carcasses, and can be used for demonstration purposes and as research tool. Comparisons using a definitive set of filters demonstrated that the contrast between feces-treated and untreated apple surfaces was greatest at 668 nm, compared to 678, 685, or 700 nm. Using the 668 nm filter, images of artificially contaminated apples taken after the apples were washed showed

that residual fluorescence responses could be detected after 5 h of feces-apple contact. No response was apparent if the contact time was less than 4 h. Use of a modified system as a teaching tool allowed public demonstration of the fact that fecal contamination invisible to the naked eye can easily be detected with appropriate instrumentation. This system has many potential uses, including investigation of the potential for fecal contamination at various stages of commercial processing of agricultural commodities. For example, the system could be used to examine the efficacy of apple washing systems.

References

Armstrong, G.L., Hollingsworth, J., Morris Jr., J.G., 1996. Emerging foodborne pathogens: *Escherichia coli O157:H7* as a model of entry of a new pathogen into the food supply of the developed world. Epidemiol. Rev. 18, 29–51.

Blackburn, C.W., McClure, P.J. (Eds.), 2002. Foodborne Pathogens: Hazards, Risk Analysis, and Control. CRC Press, Cambridge.

Food Safety Inspection Service (FSIS) 2004. Livestock post-mortem inspection activities-enforcing the zero tolerances for fecal materials, ingesta, and milk. FSIS Directive 6420.2, http://www.fsis.usda.gov.

Food and Drug Administration (FDA) 2001. Hazard analysis and critical control point (HAACP); Procedures for the safe and sanitary processing and importing of juices. Fed. Reg. 66, pp. 6137–6202.

Hui, Y.H. (Ed.), 2001. Foodborne Disease Handbook. Marcel Dekker, New York.

Kim, M.S., Lefcourt, A.M., Chen, Y.R., Kim, I., Chao, K., Chan, D., 2002. Multispectral detection of fecal contamination on apples based on hyperspectral imagery. II. Application of fluorescence imaging. Trans. ASAE 45, 2027–2038.

Kim, M.S., Lefcourt, A.M., Chen, Y.R., 2003. Optimal fluorescence excitation and emission bands for detection of fecal contamination. J. Food Protect. 66, 1198–1207.

Lefcourt, A.M., Kim, M.S., Chen, Y.R., 2003. Automated detection of fecal contamination of apples by multi-spectral laser-induced fluorescence imaging. Appl. Opt. 42, 1–9.

Mead, P.S., Slutsker, L., Dietz, V., McCaig, L.F., Bresee, J.S., Shapiro, C., Griffin, P.M., Tauxe, R.V., 1999. Food-related illness and death in the United States. Emerging Infect. Dis. 5, 607–625.

Otsu, N. 1979. A threshold selection method from gray-level histograms. IEEE Trans. Syst. Man Cybernetics SMC-9, 62–66.

Park, B., Chen, Y.R., 2001. Co-occurrence matrix texture features of multi-spectral images on poultry carcasses. J. Agric. Eng. Res. 78, 127–139.

Weeks Jr., A.R., 1996. Fundamentals of Electronic Image Processing. SPIE Optical Engineering Press, Bellington, Wash.